20. W. M. Jackson, J. B. Halpern, P. D. Feldman, J. Rahe, *Astron. Astrophys.* **107**, 385 (1982).
21. L. Haser, *Bull. Acad. R. Sci. Liège* **43**, 740 (1957). The CS_2 lifetime (500 r_h^2 s) is so short that we assume that collisions equilibrate the CS_2 and CS velocities to the same value (0.8 $r_h^{-0.5}$ km s^{-1} and 0.85 $r_h^{-0.5}$ km s^{-1} for the HST and IUE data, respectively). Examination of the relevant collision rates indicates that this assumption is justified for most of the 1996 observations but may not be valid at the larger values of r_h. Using a vectorial model raises Q_{CS_2} by a factor of ~2 relative to the Haser model result at all values of r_h. Thus, using a single model, either Haser or vectorial, does not change the power law index for the r_h variation of Q_{CS_2}. Using a vectorial model at large r_h and a Haser model at small r_h would produce a smaller power law index, which strengthens our conclusion that Q_{CS_2} and Q_{H_2O} had different variations with r_h. We assumed that a CS molecule is produced for every CS_2 molecule that is destroyed, and we used a CS lifetime of $1 \times 10^5 r_h^2$ s.
22. J. J. Cowan and M. F. A'Hearn, *Moon and Planets* **21**, 155 (1979).
23. At large r_h the activity in Hale-Bopp was apparently driven by the sublimation of CO ice (*2, 3*), which means that dust grains in the coma may have retained a H_2O ice mantle. Owing to their low efficiency at radiating heat, micrometer-sized grains can become warmer than the nucleus, which means that H_2O in the coma at large r_h could be due primarily to sublimation from these icy grains and that our values of Q_{H_2O} no longer refer to H_2O production from the nucleus. As is typically the case for comets, H_2O sublimation from the nucleus of Hale-Bopp presumably became the dominant source of H_2O in the coma at some point. Perhaps the best evidence for the latter is the agreement between our model sublimation curves and the observed values of Q_{H_2O}. The activation of several new vents on the surface of the nucleus during mid-1996, as observed in ground-based images of Hale-Bopp, may also have signaled the transition from a CO-dominated comet to a H_2O-dominated one.
24. J. Crovisier *et al.*, paper on the radio observations of Hale-Bopp presented at the 28th Annual Meeting of the Division of Planetary Sciences of the American Astronomical Society, Tucson, AZ, 22 to 26 October 1996.
25. H. A. Weaver *et al.*, *Astrophys. J.* **422**, 374 (1994).
26. Assuming that CO_2 is flowing outward from the nucleus, the production rate is given by: $Q_{CO_2} = (7.25 \times 10^{18}) v \theta r_h^2 \Delta B/g$ where g is the rate constant, $v = 0.8\ r_h^{-0.5}$ km s^{-1}, B is the observed brightness of the Cameron (1, 0) band in rayleighs, and θ is the diameter of the equivalent circular aperture of 2.4 arc sec.
27. J. Crovisier *et al.*, *Science* **275**, 1904 (1997). We recomputed Q_{CO_2} derived from the ISO observations using an outflow velocity of 0.8 $r_h^{-0.5}$ in order to be consistent with the assumptions made in analyzing the HST data.
28. M. F. A'Hearn, D. G. Schleicher, P. D. Feldman, R. L. Millis, D. T. Thompson, *Astron. J.* **89**, 579 (1984). From the HST images, we calculated $Af\rho$ using a synthetic aperture having a diameter of 2 arc sec, which is close to the effective diameter of our most commonly used FOS aperture (2.4 arc sec). We found that $Af\rho$ varied with aperture size, typically at the 10 to 30% level, probably due to temporal variability in the comet. By comparing the HST imaging and spectral data, we found empirically that $Af\rho$ near 7000 Å, the effective wavelength of the F675W filter used for the WFPC2 observations, was ~1.9 times larger than $Af\rho$ near 2950 Å. Thus, we multiplied the raw IUE $Af\rho$ values near 2950 Å by 1.9 to convert them to their equivalent "optical" values. The $Af\rho$ values were converted to a common phase angle (the sun-comet-Earth angle), ϕ, of 0° by multiplying the raw values by $10^{(0.4)(0.035)\phi}$. A different choice for the phase law is unlikely to affect our conclusions, as Hale-Bopp was observed over a narrow range in phase angle.
29. For dust having an average radius a (in micrometers), density d (in grams per cubic centimeter), geometric albedo A_p, and flowing outward from the nucleus with velocity v_{dust} (in kilometers per second), the dust mass production rate, Q_{dust} (in kilograms per second) is given by: $Q_{dust} = (0.67) a d v_{dust} Af\rho / A_p$ where $Af\rho$ is in meters. We calculated Q_{dust} using $v_{dust} = 0.13\, r_h^{-0.5}$ (*30*), $a = 10$, $d = 1$, and $A_p = 0.04$ (Table 1 and Fig. 4).
30. Z. Sekanina, *Astron. Astrophys.* **314**, 957 (1996). From a detailed analysis of the dust coma, this author derived a dust ouflow velocity (v_{dust}) of ~0.05 km s^{-1} at r_h = 6.82 AU, and we have additionally assumed that $v_{dust} = 0.05\ (r_h/6.82)^{-0.5}$.
31. C. Arpigny *et al.*, *Atlas of Cometary Spectra* (Kluwer, Dordrecht, 1997).
32. L. Kamél, *Icarus* **122**, 428 (1996) and (*14*).
33. A spectrum ending at 14:05 universal time (UT) on 23 September 1996 had essentially the same continuum flux as other spectra that were taken between 10:30 and 14:05 UT. (The spectra were not continuously recorded during this latter period because the HST periodically passes behind the Earth, at which times the comet was not visible from HST. The HST orbital period is 96 min, and observations are generally limited to a duration of ~30 min each orbit.) Following a gap in our coverage due to Earth occultation, a 2-min spectrum starting at 13:41 UT had a continuum level that was 3.4 times larger than that recorded during the earlier times. In addition, three subsequent 2-min spectra showed the continuum intensity monotonically increasing at the rate of ~1.2% min^{-1}.
34. We ruled out pointing error as the source of the observed temporal variation by verifying that the flux measured in spectra taken immediately before the outburst was essentially identical to that measured during observations spanning up to ~6.5 hours earlier. A solar-type star entering the aperture and having a visual magnitude of ~11.5 could have produced the observed increase in the continuum, but no such object was present in the cometary field. Furthermore, another object entering the aperture would not explain the observed increase in CS emission. During the outburst, the spatial distribution of the continuum became markedly more peaked towards the nucleus, which is consistent with a dust outburst originating at the nucleus of the comet.
35. For spherically symmetric outflow of dust from the nucleus with velocity v, it is easy to show that the total number of grains, n_q, in a circular aperture of radius ρ is given by $n_q = (\pi/2)\, Q_q\, \rho/v$, where Q_q is the dust production rate (in particles per second) under steady-state conditions. The number of extra dust grains, n_o, created during an outburst of duration t is given by $n_o = Q_o\, t$, where Q_o is the extra production rate above the quiescent value averaged over the duration of the outburst. Since $n_o/n_q = 2.4$, $\rho = 2570$ km, and $t = 4635$ s for our observations, the ratio of these two production rates is given by $2.1/v$ when v is in kilometers per second. Using our adopted value for v (0.076 km s^{-1}) yields a Q ratio of 28. In cometary work it is usually assumed that the dust velocity is given by $v \sim 0.5\, r_h^{-0.5}$ [N. T. Bobrovnikov, *Astron. J.* **59**, 357 (1954)], which gives a Q ratio of 7 and implies that the total dust production rate averaged over the outburst was eight times the quiescent value.
36. Assuming that all of the molecules produced during the outburst are contained in the observing aperture, the number of daughter molecules, n_d, at time t following the outburst is related to the number of parent molecules, n_p, produced during the outburst by $n_d = n_p (1 - e^{-t/\tau})$, where τ is the parent lifetime. Using our adopted lifetimes for CS_2 and H_2O, and an outburst duration of 4635 s, we see that the increase in the number of CS molecules should be ~64% of the increase in the number of CS_2 molecules, while the number of extra OH molecules should increase by less than 1% of the increase in H_2O molecules.
37. Support for this work was provided by NASA through grant numbers GO-05844 and GO-06663 from the Space Telescope Science Institute (STScI), which is operated by the Association of Universities for Research in Astronomy, Inc., under NASA contract NAS5-26555. C. Arpigny gratefully acknowledges financial support by the Belgian Fonds National de la Recherche Scientifique. We thank A. Lubenow and A. Storrs of the STScI for expertly planning the HST observations of Hale-Bopp. We also express our gratitude to W. Wamsteker and H. Andernach for their strong support of the IUE Hale-Bopp program.

28 January 1997; accepted 3 March 1997

The Spectrum of Comet Hale-Bopp (C/1995 O1) Observed with the Infrared Space Observatory at 2.9 Astronomical Units from the Sun

Jacques Crovisier,* Kieron Leech, Dominique Bockelée-Morvan, Timothy Y. Brooke, Martha S. Hanner, Bruno Altieri, H. Uwe Keller, Emmanuel Lellouch

Comet Hale-Bopp (C/1995 O1) was observed at wavelengths from 2.4 to 195 micrometers with the Infrared Space Observatory when the comet was about 2.9 astronomical units (AU) from the sun. The main observed volatiles that sublimated from the nucleus ices were water, carbon monoxide, and carbon dioxide in a ratio (by number) of 10:6:2. These species are also the main observed constituents of ices in dense interstellar molecular clouds; this observation strengthens the links between cometary and interstellar material. Several broad emission features observed in the 7- to 45-micrometer region suggest the presence of silicates, particularly magnesium-rich crystalline olivine. These features are similar to those observed in the dust envelopes of Vega-type stars.

The infrared (IR) wavelength region is useful for investigating comets because (i) comets are cold and the thermal emission of the nucleus and dusty atmosphere peaks at IR wavelengths and (ii) the volatile molecular species, sublimated from cometary nucleus ices, can be identified through their fundamental bands of vibration, which are seen in fluorescence excited by solar radiation. IR observations of comets (*1–3*) from the ground are limited to a few atmospheric windows. IR spectra of comets above Earth's atmosphere

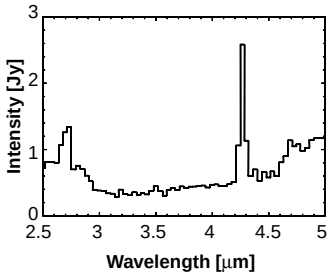

Fig. 1. The 2.5- to 5-μm spectrum of Hale-Bopp observed with PHT-S on 27 September 1996. The aperture is 24 arc sec × 24 arc sec and the spectral resolution is λ/δλ ~ 90. Conspicuous are the bands of H_2O at 2.7 μm, CO_2 at 4.25 μm, and CO at 4.65 μm.

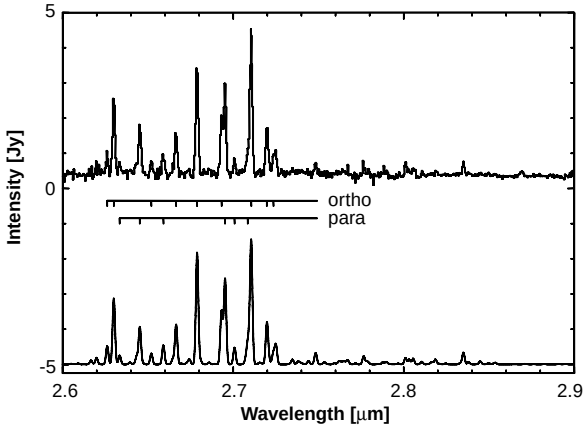

Fig. 2. (Top) The 2.6- to 2.9-μm spectrum of Hale-Bopp observed with the SWS, an average of the 27 September and 6 October 1996 data. The aperture is 14 arc sec × 20 arc sec and the spectral resolution is λ/δλ ~ 1500. (Bottom) The synthetic fluorescence spectrum of water for $Q_{H_2O} = 3.6 \times 10^{29}$ s^{-1}, T_{rot} = 28.5 K, and OPR = 2.45, which is the best fit to the data. All the observed lines are due to water, except the line at 2.869 μm which is identified to the OH v(1-0) P_1 (5/2) transition. The *ortho* and *para* lines of the ν_3 band of water are tagged.

have been observed for comet Halley, from the VEGA space probes, and from the Kuiper Airborne Observatory (*4–7*), but they were limited in spectral coverage, resolution, or both. Hale-Bopp, an intrinsically bright long-period comet ($P \sim 2500$ years) that will reach perihelion at 0.91 AU on 1 April 1997, provides a rare opportunity to measure the whole IR spectrum of a comet with good spectral resolution and sensitivity, by use of the Earth-orbiting Infrared Space Observatory (ISO).

Our observations (*8*) were performed with the grating spectrometer of the photometer (PHT-S, wavelengths of 2.5 to 5 and 6 to 12 μm), the short-wavelength spectrometer (SWS, 2.4 to 45 μm), and the long-wavelength spectrometer (LWS, 45 to 195 μm) on board ISO (*9*). The 2.5- to 5-μm spectral region covers the most intense fundamental vibrational bands of cometary volatiles which are emitted through fluorescence (*1*). This region was observed at low resolution with PHT-S. In April, only the ν_3 band of CO_2 at 4.25 μm was detected (*10*). On 27 September and 6 October, we detected the ν_3 band of CO_2 with a high signal-to-noise ratio (SNR), the H_2O band at 2.7 μm, and the CO v(1-0) band (Fig. 1) (*11*). These bands were also observed at higher spectral resolution with the SWS (*12*). The CO and CO_2 bands were seen with a lower SNR compared to the PHT-S spectra due to the limited sensitivity of the SWS detectors at these wavelengths. The 3.2- to 3.6-μm emission, which is a major feature of comets observed at ~1 AU and is attributed to methanol (CH_3OH), ethane (C_2H_6), and other unidentified species (*3, 13*), was only detected in the SWS spectra.

J. Crovisier, D. Bockelée-Morvan, E. Lellouch, Observatoire de Paris-Meudon, F-92195 Meudon, France.
K. Leech and B. Altieri, ISO Science Operations Centre, Astrophysics Division of European Space Agency, Post Office Box 50727, E-28080 Villafranca, Spain.
T. Y. Brooke and M. S. Hanner, Jet Propulsion Laboratory, 4800 Oak Grove Drive, Pasadena, CA 91109, USA.
H. U. Keller, Max Planck Institut für Aeronomie, Postfach 20, D-37189 Katlenburg-Lindau, Germany.

*To whom correspondence should be addressed. E-mail: crovisie@obspm.fr

The gas production rates Q for H_2O, CO_2, and CO were evaluated assuming resonant fluorescence excited by the sun (Table 1) (*1, 14*). We assumed optically thin gas flowing isotropically at constant velocity [0.5 km s^{-1} in April and 0.7 km s^{-1} in September (*15*)] and standard photodissociation lifetimes (*16*). These parameters are fairly well known, and the principal source of error in the gas production rates is probably the ~30% uncertainty in the flux calibration.

Other determinations of the production rates of CO and H_2O (from OH) at radio wavelengths and in the ultraviolet with the Hubble Space Telescope are similar to our estimates (*17*). The production rates of CO and CO_2 relative to H_2O at large heliocentric distances (r_h) where Hale-Bopp was observed may not be representative of the true mixing ratios in the nucleus because of the high volatility of these species. Numerical simulations (*18*) have been used to evaluate this fractionation effect, which appears to be important at $r_h = 4.6$ AU. At $r_h = 2.9$ AU, the [CO]/[H_2O] and [CO_2]/[H_2O] measured in the coma of Hale-Bopp could be closer to the mixing ratios of the nucleus ices, but may still be an overestimate. In any case, H_2O, CO, and CO_2 appear to be the main observed constituents of cometary ices. Other constituents have relative abundances of the order of a few percent, at most (*15, 19*). In this respect, the composition of cometary ice appears to be very similar to that of interstellar ice observed by ISO (*20*).

On 27 September and 6 October, specific SWS observations were dedicated to the 2.6- to 2.9-μm spectral region, which contains bands of water (ν_1, ν_3, and several hot bands), as well as the O-H stretching modes of several molecules (Fig. 2). The strong lines observed between 2.62 and 2.73 μm belong to the ν_3 H_2O band, resolved into its ro-vibrational lines. The 2.73- to 2.90-μm region shows several weak lines. Using a fluorescence model of H_2O (*14, 21*), we computed a synthetic spectrum that takes into account excitation of the ν_1 and ν_3 fundamental bands and of the $\nu_2 + \nu_3 - \nu_2$, $\nu_1 + \nu_3 - \nu_1$, and $\nu_1 + \nu_3 - \nu_3$ hot bands of H_2O. There is a good match with the observed weak features (Fig. 2). This confirms that the cometary emission around 2.8 μm, previously found in Halley and comet Wilson (C/1986 P1) (*22*), is mainly due to H_2O (*21*). An additional line observed at 2.869 μm corresponds to the v(1-0) P_1 (5/2) transition of OH. The fluorescence of this line was predicted to be strong, together with the v(1-0) Q_1 (3/2) line at 2.803 μm, which appears in our spectrum to be blended with H_2O lines (*23*).

The lines of the ν_3 H_2O band are observed with high SNR. Their relative intensities are sensitive to the physical conditions of cometary water. They allow us to measure the H_2O rotational temperature (T_{rot}) and its *ortho*-to-*para* ratio (OPR), a tracer of the origin and evolution of comets (*24*). Using our model (*14, 21*), we solved by a least-square method for the production rate, the OPR and T_{rot} which give the best fit to the observed spectrum (Fig. 2). We assumed that the rotational population distributions for both *para* and *ortho* states can be described by a single T_{rot} and we took opacity effects into account (*14*). The

Table 1. Molecular production rates from PHT-S spectra. Upper limits are 3-σ. All these results are subject to a 30% uncertainty on the calibration. The band for H_2O and CO_2 is ν_3 and the band for CO is v(1-0). The g-factors (fluorescence efficiency, in s^{-1}) are as follows: H_2O, 2.9×10^{-4}; CO_2, 2.6×10^{-3}; CO, 2.6×10^{-4}. Molec. indicates molecule.

Molec.	Flux (W m^{-2})	Q (Molec. s^{-1})
27 Apr. 1996: $r_h = 4.59$ AU, $\Delta = 4.28$ AU		
H_2O	$<2.6 \times 10^{-15}$	$<1.1 \times 10^{29}$
CO_2	2.1×10^{-15}	1.3×10^{28}
CO	$<1.2 \times 10^{-15}$	$<9.0 \times 10^{28}$
27 Sept. 1996: $r_h = 2.93$ AU, $\Delta = 2.96$ AU		
H_2O	2.0×10^{-14}	3.3×10^{29}
CO_2	2.7×10^{-14}	7.4×10^{28}
CO	6.7×10^{-15}	2.3×10^{29}*

*subject to baseline uncertainty.

retrieved T_{rot} is 28.5 K, in agreement with the temperatures derived from the radio lines of other species (*15*). The OPR is 2.45 ± 0.10 and is significantly lower than the statistical equilibrium value of 3, achieved for temperatures exceeding ~60 K. Such a value suggests that cometary H_2O molecules formed at a temperature of ~25 K and were not subject to subsequent re-equilibration (*25*).

Water was also observed at 6 μm by the SWS through the ro-vibrational lines of its ν_2 band. In addition, the far-IR LWS spectrum (Fig. 3) shows emission of the 2_{12}-1_{01} rotational line of water [the 2_{21}-2_{12} H_2O line falls at a very close wavelength; its intensity in cometary atmospheres is expected to be much smaller, however (*14*)]. The 3_{03}-2_{12} H_2O line is also marginally present. These lines are, as predicted (*1, 14*), the strongest cometary lines in this spectral domain. Acting as coolers, they have an important role in the thermal balance of cometary atmospheres.

The 7- to 45-μm region observed with the SWS on 6 October (the spectrum obtained on 27 September is almost identical) shows continuum and strong emission features at 10 to 12, 19.5, 23.5, and 33.5 μm; less intense features are also seen at 16 and 27.5 μm (Fig. 4). The spectrum represents thermal emission from the dust grains in the coma. A temperature of 200 K was derived by fitting a black-body curve to the spectrum at 7.5 and 13 to 15 μm (Fig. 4). The fitted black-body temperature is ~20% higher than the calculated equilibrium black-body temperature of 162 K at r_h = 2.9 AU, indicating that the thermal emission arises from particles that are small compared to the wavelength.

The spectral peaks may be indicative of minerals within the dust particles. The emission feature at a wavelength of 9 to 12 μm has been observed from the ground for a number of comets at spectral resolution ~50 (*2, 5*), including Hale-Bopp (*26*). This band may be due to the stretching mode of Si-O in small silicate grains. Several of the comets, including Hale-Bopp, exhibit a distinct peak at 11.3 μm superimposed on a broader emission; this peak may be attributed to crystalline olivine (*2*). Amorphous silicates have only broad bands around 10 and 20 μm (*27*). The broad excess emission at 16 to 26 μm in our spectrum is typical of silicates (*27–30*), regardless of specific mineralogy. Crystalline olivine (Mg, Fe)$_2$SiO$_4$ has additional bands at 16.5, 19.8, 24.0, 27.6, and 33.9 μm (*28, 29*). Crystalline pyroxene (Mg, Fe, Ca)SiO$_3$ has bands at 15.6, 26.5, 29.5, 37.5, and 49 μm (*30*) (there is some variation in peak positions among the pyroxenes, but none of the peaks are the same as those of olivine). Thus, all the emission features observed in the 6- to 45-μm spectrum of Hale-Bopp appear to correspond to those of crystalline olivine rather than pyroxene. A detailed comparison with the spectra obtained for a series of olivines with various Mg/Fe ratios (*28*) reveals that the peaks of the Hale-Bopp spectrum match those of the Mg-rich olivine (forsterite) more precisely. A Mg-rich composition is consistent with the wavelength of the 11.3-μm peak and with the dust particle composition measured during the Halley fly-bys (*31*).

Until now, the nature of cometary dust has been a debated issue primarily on the basis of analysis of the shape of the 9- to 12-μm emission observed from the ground (*2, 5, 29*). The only previous spectra at longer wavelengths were from airborne observations of Halley at 1.2 to 1.4 AU, with a resolution of ~100 (*7*) or ~25 (*6*). A peak at 28.4 μm is present in the first spectrum with possible features at 17, 19.5, and 23.8 μm (*7*); these peaks are hardly visible in the other spectra (*6*). They were tentatively attributed to crystalline silicates. The Hale-Bopp ISO spectrum now suggests that the dust of this comet contains crystalline silicates, and particularly Mg-rich olivine.

Recent ISO observations of the circumstellar disks of Vega-type stars have revealed that the dust shells around these stars also contain crystalline silicates (*32, 33*). Crystalline silicates were suggested from analysis of the 10- to 12-μm emission of β Pic (*34*). Indeed, the spectrum of HD 100546 (an intermediate star between Herbig Ae/Be stars and Vega-like objects) shows features similar to those in Fig. 4 (*32*). The similarity of these spectra with our spectra of Hale-Bopp establishes a possible link between the primordial solar system dust preserved in comets and the dust around young stars. It has even been suggested that the grains in HD 100546 are being released from cometary bodies colliding with the central star (*35*).

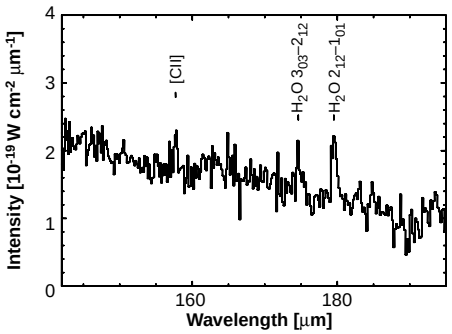

Fig. 3. The rotational water lines observed in Hale-Bopp with the LWS on 6 October 1996. The aperture is 100 arc sec and the spectral resolution is λ/δλ ~ 200. The [CII] line at 157.7 μm, also present in the same field observed several days later, is probably due to emission originating in the background interstellar medium.

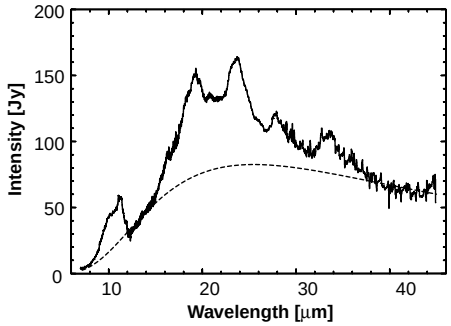

Fig. 4. The 7- to 45-μm spectrum of Hale-Bopp observed with the SWS on 6 October 1996. The spectral resolution has been degraded to λ/δλ ~ 500. The ripples in the 12- to 28-μm region are instrumental (caused by interferences at the surface of the detectors). The instrumental aperture is 14 arc sec × 20 arc sec up to 12 μm, 14 arc sec × 27 arc sec from 12 to 29 μm, and 20 arc sec × 33 arc sec above 29 μm. The subspectra obtained in the different bands of the instrument, which were offset with respect to one another due to different instrumental apertures and to calibration uncertainties, have been scaled to the 6- to 12-μm band to obtain a continuous spectrum. The dotted line shows a black-body curve fitted to 7.5 and 13 to 15 μm.

REFERENCES AND NOTES

1. J. Crovisier, in *Infrared Astronomy with ISO*, T. Encrenaz and M. F. Kessler, Eds. (Nova Science, New York, 1992), pp. 221–248.
2. H. Campins and E. V. Ryan, *Astrophys. J.* **341**, 1059 (1989); M. S. Hanner, D. K. Lynch, R. W. Russell, *ibid.* **425**, 274 (1994).
3. M. J. Mumma *et al.*, *Science* **272**, 1310 (1996).
4. M. J. Mumma, H. A. Weaver, H. P. Larson, D. S. Davis, M. Williams, *ibid.* **232**, 1523 (1986); M. Combes *et al.*, *Icarus* **76**, 44 (1988).
5. J. D. Bregman *et al.*, *Astron. Astrophys.* **187**, 616 (1987).
6. W. Glaccum, S. H. Moseley, H. Campins, R. F. Loewenstein, *ibid.*, p. 635.
7. T. Herter, H. Campins, G. E. Gull, *ibid.*, p. 629.
8. The comet could be observed by ISO during two visibility windows: in April 1996 when r_h = 4.6 AU (*10*) and in September and October 1996 when r_h ~3 AU. It unfortunately could not be observed closer to the sun, because ISO cannot operate at solar elongations smaller than 60°.
9. M. F. Kessler *et al.*, *Astron. Astrophys.* **315**, L27 (1996); P. Clegg *et al.*, *ibid.*, p. L38; T. de Graauw *et al.*, *ibid.*, p. L49; D. Lemke *et al.*, *ibid.*, p. L64.
10. J. Crovisier *et al.*, *ibid.*, p. L385.
11. The field of the 6 October observation was also observed several days later with PHT-S to check that no emission was coming from the background.
12. The SWS observations consisted on 27 September and 6 October of a full 2.4- to 45-μm spectral scan and a dedicated observation of the 2.6- to 2.9-μm region. On 6 October, when the comet was at r_h = 2.82 AU and Δ = 3.01 AU, dedicated observations of regions centered on 3.3, 4.5, and 6 μm were made in addition.
13. D. Bockelée-Morvan, T. Y. Brooke, J. Crovisier, *Icarus* **116**, 18 (1995).
14. D. Bockelée-Morvan, *Astron. Astrophys.* **181**, 169 (1987).
15. N. Biver *et al.*, *Science* **275,** 1915 (1997).
16. W. F. Huebner, J. J. Keady, S. P. Lyon, *Astrophys. Space Sci.* **195**, 1 (1992).
17. Production rates in April were Q_{H_2O} = 2.5 × 10^{28}

s^{-1} from the Hubble Space Telescope [H. A. Weaver *et al., Bull. Am. Astron. Soc.* **28**, 1094 (1996)] and 1.4×10^{28} s^{-1} from the radio (*15*), $Q_{CO} = 4.0 \times 10^{28}$ s^{-1} (*15*). At the end of September, $Q_{H_2O} = 6 \times 10^{29}$ s^{-1} and $Q_{CO} = 1.6 \times 10^{29}$ s^{-1} (*15*). The higher radio Q_{H_2O} may be due to calibration and model uncertainties, or to comet variability.

18. S. Espinasse, J. Klinger, C. Ritz, B. Schmitt, *Icarus* **92**, 350 (1991); J. Benkhoff and W. F. Huebner, *ibid.* **114**, 348 (1995); M. T. Capria *et al.*, *Planet. Space Sci.* **44**, 987 (1996).
19. J. Crovisier, in *Asteroids, Comets, Meteors 1993*, A. Milani *et al.,* Eds. (Kluwer, Dordrecht, Netherlands, 1994), pp. 149–173; D. Bockelée-Morvan, in *IAU Symposium 178, Molecules in Astrophysics: Probes and Processes*, E. van Dishoeck, Ed. (Kluwer, Dordrecht, in press).
20. L. d'Hendecourt *et al.*, *Astron. Astrophys.* **315**, L365 (1996); D. C. B. Whittet *et al.*, *ibid.*, p. L357.
21. D. Bockelée-Morvan and J. Crovisier, *ibid.* **216**, 278 (1989).
22. A. T. Tokunaga, T. Nagata, R. G. Smith, *ibid.* **187**, 519 (1987); H. A. Weaver, M. J. Mumma, H. P. Larson, S. Drapatz, in *The Formation and Evolution of Planetary Systems*, Space Telescope Science Institute (STScI) Workshop (1988); T. Y. Brooke, R. F. Knacke, T. C. Owen, A. T. Tokunaga, *Astrophys. J.* **336**, 971 (1989).
23. D. G. Schleicher and M. F. A'Hearn, *Astrophys. J.* **331**, 1058 (1988).
24. Water exists in two spin species, *ortho* and *para*. Conversion between these two species, either radiatively or through collisions, is forbidden. It is thus believed that its OPR is determined by the temperature at which water was formed and was then preserved [M. J. Mumma, H. A. Weaver, H. P. Larson, *Astron. Astrophys.* **187**, 419 (1987)]. OPRs are thus indicative of the original temperature of cometary material and constrain cometary formation scenarios.
25. OPRs of 2.2 ± 0.1 and 3.2 ± 0.2 were derived for Halley and Wilson, respectively; it was suggested that this latter value may indicate significant cosmic-ray damage in the outer layers of new comets coming from the Oort cloud [M. J. Mumma, W. E. Blass, H. A. Weaver, H. P. Larson, in *The Formation and Evolution of Planetary Systems*, STScI Workshop (1988)]. It was argued [D. Bockelée-Morvan and J. Crovisier, in *Asteroids, Comets, Meteors III* (Uppsala University, Uppsala, Sweden, 1990), pp. 263–265] that the OPR derived in Halley may have been underestimated by assuming optically thin lines. Because of the lower H_2O production rate and of the larger geocentric distance of comet Hale-Bopp, the opacity effects are less important in our ISO spectrum; they were estimated to change the intensities of the stronger lines by less than 10%.
26. T. L. Hayward and M. S. Hanner, *Science* **275**, 1907 (1997).
27. C. Koike and A. Tsuchiyama, *Mon. Not. R. Astron. Soc.* **255**, 248 (1992); J. Dorschner, B. Begemann, T. Henning, C. Jäger, H. Mutschke, *Astron. Astrophys.* **300**, 503 (1995).
28. C. Koike, H. Shibai, A. Tuchiyama, *Mon. Not. R. Astron. Soc.* **264**, 654 (1993).
29. L. Colangeli, V. Mennella, C. Di Marino, A. Rotundi, E. Bussoletti, *Astron. Astrophys.* **293**, 927 (1995).
30. C. Jäger, H. Mutschke, B. Begemann, J. Dorschner, T. Henning, *ibid.* **292**, 641 (1994).
31. E. K. Jessberger and J. Kissel, in *Comets in the Post-Halley Era*, R. L. Newburn *et al.* Eds. (Kluwer, Dordrecht, Netherlands, 1991), pp. 1075–1092; M. E. Lawler, D. E. Brownlee, S. Temple, M. M. Wheelock, *Icarus* **80**, 225 (1989).
32. C. Waelkens *et al.*, *Astron. Astrophys.* **315**, L245 (1996).
33. L. B. F. M. Waters *et al.*, *ibid.*, p. L361.
34. R. G. Knacke *et al.*, *Astrophys. J.* **418**, 440 (1993).
35. C. A. Grady *et al.*, *ibid.*, in press.
36. This study was based on observations with ISO, a European Space Agency (ESA) project with instruments funded by ESA Member States (especially the principal investigator countries: France, Germany, the Netherlands, and the United Kingdom) and with participation of ISAS and NASA. The ISOPHOT data presented in this paper were reduced using PIA (Interactive Analysis Package), which is a joint development by the ESA Astrophysics Division and the ISOPHOT consortium led by the Max Planck Institute für Astronomie, Heidelberg. We thank P. Rocher and the Bureau des longitudes, Paris, for providing ephemeris of the comet.

4 February 1997; accepted 27 February 1997

Ground-Based Thermal Infrared Observations of Comet Hale-Bopp (C/1995 O1) During 1996

T. L. Hayward and M. S. Hanner

Thermal infrared (IR) imaging and spectroscopy of comet Hale-Bopp (C/1995 O1) during June, August, and September 1996 traced the development of the dust coma several months before perihelion. Images revealed nightly variations in the brightness of the inner coma from 1 to 12 June that were correlated with the appearance of a northward-pointing jet. The central IR flux increased by a factor of 8 between 1 June and 30 September, and the September data showed IR jets that corresponded to similar structures that were visible in reflected sunlight at shorter wavelengths. At all epochs, 8- to 13-micrometer spectra of the central coma revealed a strong silicate emission feature, including an 11.2-micrometer feature indicative of crystalline olivine, even when the comet was at a heliocentric distance of 4.1 astronomical units.

Comet Hale-Bopp (C/1995 O1) has provided a rare opportunity for observation of a bright, active comet at large heliocentric distances. The comet's high intrinsic brightness is particularly important to IR studies of thermal emission from cometary dust grains because the thermal background radiation from a warm ground-based telescope limits sensitivity. Most comets can thus be studied in detail only when they are within 1 or 2 astronomical units (AU) of the sun, where their dust grains are relatively warm. Hale-Bopp, however, could be detected easily in the thermal IR when it was still far from the sun and its grains were relatively cool. Also, recent advances in two-dimensional array detectors sensitive to IR radiation at wavelengths between 5 and 30 μm allow study of comets at an angular resolution comparable to that of optical and near-IR observations. Here we present 8- to 13-μm images and spectra of Hale-Bopp that were taken with a modern array camera/spectrograph during the summer and fall of 1996, when the comet was still more than 6 months from perihelion.

We observed Hale-Bopp using the SpectroCam-10 imaging spectrograph (*1*, *2*) on the 5-m Hale telescope at Palomar Observatory (*3*) during three observing runs: 1 to 12 June 1996 (when the comet was at a heliocentric distance $r_h = 4.2$ AU and a geocentric distance $\Delta = 3.3$ AU), 4 to 7 August ($r_h = 3.5$ AU, $\Delta = 2.7$ AU), and 28 to 30 September ($r_h = 2.9$ AU, $\Delta = 3.0$ AU). The comet was observed at least briefly each night except for 3 June. We imaged Hale-Bopp through 1-μm bandpass filters spaced across the 10-μm atmospheric window in order to measure the comet's overall brightness and morphology (Fig. 1). At wavelength (λ) = 10.3 μm, the inner coma region within a circle 3 arc sec in diameter centered on the nucleus brightened from 1 to 8 Janskys (Jy) between 1 June and 30 September. This change was greater by a factor of 2 to 4 than the approximately 1 to 1.5 magnitude increase in the total visual magnitude reported during this period, due in part to the increasing temperature of the grains. The general brightening was punctuated by a number of outbursts; during some outbursts, the comet's brightness within the 3-arc-sec circle increased by a factor of 2. Similar short-term brightness increases were observed in comet P/Halley (*4*). A short-term change in the dust production rate would be expected to cause a larger percentage change in the brightness of the inner few arc seconds than in the brightness of the entire coma (*4*).

On 2 June, when Hale-Bopp was at a typical inter-outburst brightness, the inner coma was nearly symmetric (Fig. 1A). During the first observed outburst on 4 June, a prominent northward-pointing jet appeared (Fig. 1B). The jet varied noticeably from night to night through the remainder of the June run. By August, the jet had evolved into the broader fan that was familiar from optical images (Fig. 1C). In September (Fig. 1D), we detected as many as five jets that appeared to be the thermal IR counterparts of jets seen in reflected sunlight in the optical and near-IR, including a jet pointing to the west, in the direction of the sun. In the 28 September image, the brightness within synthetic apertures of increasing di-

T. L. Hayward, Center for Radiophysics and Space Research, Cornell University, Ithaca, NY 14853, USA. E-mail: hayward@astrosun.tn.cornell.edu
M. S. Hanner, Jet Propulsion Laboratory, California Institute of Technology, 4800 Oak Grove Drive, Pasadena, CA 91109, USA. E-mail: msh@scn1.jpl.nasa.gov